

# Do ULXs Really Contain Intermediate-mass Black Holes?

Kiki VIERDAYANTI<sup>1</sup>, Shin MINESHIGE<sup>1</sup>, Ken EBISAWA<sup>2</sup> and Toshihiro KAWAGUCHI<sup>3</sup>

<sup>1</sup> Yukawa Institute for Theoretical Physics, Kyoto University, Sakyo-ku, Kyoto 606-8502

<sup>2</sup> Institute of Space and Astronautical Science, Japan Aerospace Exploration Agency (ISAS/JAXA),  
 Yoshinodai 3-1-1, Sagamihara, Kanagawa, 2298510, Japan

<sup>3</sup> Department of Physics and Mathematics, Aoyama Gakuin University, Kanagawa, 229-8558  
 kiki@yukawa.kyoto-u.ac.jp

(Received 2006 July 21; accepted 2006 August 24)

## Abstract

It still remains an open question if the Ultraluminous X-ray Sources (ULXs) really contain intermediate-mass black holes (IMBHs). To settle down this vital issue, we have carefully investigated the XMM-Newton EPIC spectra of the four ULXs which were claimed as strong candidates of IMBHs by several authors. We first tried fitting by the standard spectral model of disk blackbody (DBB) + power-law (PL), finding good fits to all the data, in agreement with others. We, however, find that the PL component dominates the DBB component at  $\sim 0.3$  to 10 keV. Thus, the black hole parameters derived solely from the minor DBB component are questionable. Next, we tried to fit the same data by the “*p*-free disk model” without the PL component, assuming the effective temperature profile of  $T_{\text{eff}} \propto r^{-p}$  where  $r$  is the disk radius. Interestingly, in spite of one less free model parameters, we obtained similarly good fits with much higher innermost disk temperatures,  $1.8 < kT_{\text{in}} < 3.2$  keV. More importantly, we obtained  $p \sim 0.5$ , just the value predicted by the slim (super-critical) disk theory, rather than  $p = 0.75$  that is expected from the standard disk model. The estimated black hole masses from the *p*-free disk model are much smaller;  $M \lesssim 40M_{\odot}$ . Furthermore, we applied the more sophisticated slim disk model by Kawaguchi (2003) and obtained good fits with roughly consistent black hole masses. We thus conclude that the central engines of these ULXs are super-critical accretion flows to stellar-mass black holes.

**Key words:** accretion, accretion disks — black hole physics — X-rays: individuals (NGC 5204 X-1, NGC 4559 X-7, NGC 4559 X-10, NGC 1313 X-2) — X-rays: stars

## 1. Introduction

X-ray data analysis has become one of the most widely studied subjects in these days, and made great contributions in the progress of astrophysics. This is particularly true in the field of astrophysical black holes. Thanks to the rapid improvement of the sensitivity of X-ray detectors, new types of X-ray sources have been discovered. Some of them seem to be black holes which were not known before.

Recent X-ray observations on many nearby spiral galaxies showed that the X-ray radiation consists of emission from several discrete X-ray sources, such as hot gaseous media, active galactic nucleus (AGN) and the point-like off-center X-ray sources whose X-ray luminosities significantly exceed the Eddington luminosity of a neutron star (Fabbiano 1989). The bright point-like off-center X-ray sources which cannot be identified with young supernova remnants are known as ultraluminous X-ray sources (ULXs; e.g., Makishima et al. 2000; Ptak, Colbert 2004). The ULXs, despite the fact of being very luminous ( $L_x \sim 10^{39-41} \text{ ergs}^{-1}$ ), cannot be explained as collections of many sources with each luminosity less than the Eddington limit, since many of the ULXs exhibit significant time variabilities (e.g., Makishima et al. 2000). Therefore, one reasonable assumption is that the ULXs are single compact objects powered by accretion flow.

Then, how can we understand the extremely large luminosities exceeding the Eddington luminosity for a mass of  $\sim 10 M_{\odot}$ ?

A possibility that ULXs are only bright toward our line of sights (beaming model) was proposed (e.g. King et al. 2001, Körding et al. 2002, Reynolds et al. 1997), but is not generally accepted now. In fact, Wang (2002) has shown the existence of a bright nebula surrounding the ULX M81 X-9, and some ULXs also exhibit extended optical nebulae (Pakull, Mirioni 2002). There is an evidence that some ULXs are associated with a spreading wave of star formation, which supports the idea that many ULXs, in particular those located in star forming galaxies, are high mass X-ray binaries (King 2004). These facts indicate that the ULX surrounding nebulae are powered by the central high mass X-ray sources, and that strong X-ray beaming toward our direction is unlikely.

Then, the question is, how massive the central compact objects are. At present, there are basically two distinct lines of thoughts: sub-Eddington accretion onto an intermediate (several hundreds  $M_{\odot}$ ) mass black hole (IMBH), and super-Eddington (super-critical) accretion onto a stellar-mass black hole. The success in fitting several ULXs spectra with a multicolor disk blackbody (DBB) and a power-law (PL) model supports the idea of IMBHs for the ULXs (Miller et al. 2003, Miller et al. 2004;

Cropper et al. 2004, Roberts et al. 2005), since the cool inner disk temperatures and the large innermost radii, obtained through model fitting, suggests a black hole mass within the IMBH range. The other line of thoughts, supporting a super-Eddington accretion flow, is the slim disk model with stellar mass black holes (Watarai et al. 2001; Kawaguchi 2003, Ebisawa et al. 2003; Okajima et al. 2006). The present article concerns with the super-Eddington thick accretion disks introduced in the early 1980s by the Warsaw group and their collaborators (e.g. Abramowicz et al. 1978; Abramowicz et al. 1980) and with the slim accretion disks, introduced in the late 1980s by the Warsaw and the Kyoto groups (Abramowicz et al. 1988, Abramowicz et al. 1989). In these papers, the very possibility of the super-Eddington beaming in the thick accretion disk funnels, crucial for arguments presented here, was explicitly recognized, discussed and stressed.

The IMBH notion faces a serious problem that the formation of IMBH itself remains unsettled (e.g., Madhusudhan et al. 2006). In contrast, the alternative possibility of the super-critical accretion has been poorly investigated so far due mainly to our limited knowledge about properties of the super-critical flow. The situation has been remarkably improved in the past few years, however, since the basic tools for investigating high-luminosity accreting systems are now available. In the present paper, we investigate the XMM-Newton EPIC spectra of the four ULXs which had been claimed as strong IMBH candidates, using theoretical super-critical models to see whether the super-critical accretion takes place in these ULXs or not. Our final goal is to determine the mass of the central black holes and settle down the issue regarding the origin of ULXs.

We apply accretion disk spectral models to the observed ULX energy spectra, constrain the innermost disk radius, and estimate the black hole mass. A very similar method as the one used in the present paper was successfully applied to Galactic black hole binaries (e.g., Ebisawa et al. 1991; Ebisawa et al. 1993; Gierliński et al. 2001). Several authors have recently done elaborate mass and angular momentum estimates by spectral fitting for microquasars, i.e. by a very similar method as the one used in the present paper (Shafee et al. 2006; McClintock et al. 2006; Davis et al. 2006). In the present study, however, we focus on the mass estimation and do not attempt to estimate the spin of the black hole.

The mass of the ULXs can also be accurately estimated by a different method than that described in our article. For this other independent estimate, double peak QPOs in the 3:2 resonance should be detected in ULXs (Abramowicz et al. 2004). This is because these QPOs scale inversely with the mass of the source, which was first shown for microquasars by McClintock and Remillard (2003), and more recently for low-mass Seyfert galaxies by Lachowicz et al. (2006). There is also an indication that the same scaling is true for a (possible) detection of double peak 3:2 QPOs in SgrA\* (Török 2005), while for the ULXs, in general, it has not been detected yet. According to Mucciarelli et al. (2006), the only ULX

where a QPO has been discovered at present is M82 X-1. Scaling the frequency inversely to the BH mass, the observed QPO frequency range (from a few tens to a few hundreds mHz) would yield a black hole mass anywhere in the interval from a few tens to a few thousands solar mass (Strohmayer, Mushotzky 2003; Mucciarelli et al. 2006).

Plan of this paper is as follows: We first describe the X-ray data which we used in the present study and our methods of fitting in Section 2. In Section 3, we then give the results of fitting, together with their implications on the black hole mass and mass accretion rates. Section 4 is devoted to discussion, and the final Section 5 is to conclude the paper.

## 2. Data and Fitting Methods

### 2.1. Data

We perform spectral analysis of four ULXs by using XMM-Newton observational data. The data were extracted using the XMM-Newton SAS version 6.5.0 tools. Detail extraction process will be explained separately for each object. Response files were made using the SAS tools rmfgen and arfgen for all the data.

#### 2.1.1. NGC 5204 X-1

NGC 5204 X-1 is located  $\sim 0.3$  kpc from the center of a nearby,  $D = 4.8$  Mpc, Magellanic-type galaxy (Roberts, Warwick 2000). The typical X-ray luminosity of this source is of the order of  $2 \sim 6 \times 10^{39}$  erg s $^{-1}$  (0.5 – 8 keV) (Roberts et al. 2005).

NGC 5204 X-1 data for our analysis were obtained on 2003 January 6 (observation ID 0142770101). Following Roberts et al. (2005), we set flag = 0 and pattern  $\leq 4$  for pn data, while #XMMEA\_EM flag and pattern  $\leq 12$  were used for the MOS data. No time filters were applied to the data since the background is less than 10 count s $^{-1}$  in the pn detector. Source spectra and light curves were extracted in 36 – arcsec radius circle centered on the source and 44 – arcsec radius region nearby was used to produce background data.

#### 2.1.2. NGC 4559 X-7 and X-10

NGC 4559 X-7 and X-10 are two brightest sources in NGC 4559 ( $D = 9.69$  Mpc). X-7 was located at the outer spiral arms, while X-10 was about 0.3 kpc from the optical nucleus of NGC 4559. They are also known as X1 and X4 respectively in Roberts and Warwick (2000), and IXO65 and IXO66 in Colbert and Ptak (2002) respectively (Cropper et al. 2004).

The data were obtained on 2003 May 27 (observation ID 0152170501) for both X-7 and X-10. However, X-10 was only seen in EPIC-pn since the EPIC-MOS cameras were operated in small window mode. Following Cropper et al. (2004), we used 30 – arcsec radius centered to the source for X-7, while for X-10 we used 20 – arcsec radius with an exclusion of 6 – arcsec radius centered on the nucleus of the galaxy ( $12^h35^m57.^s64$ ;  $+27^\circ57'35''$ , J2000.0). Source free region on the same CCD was selected as background for the EPIC-pn data while region as close as possible to the source were selected for EPIC-MOS X-7 data. The MOS data were filtered using pattern

$\leq 12$  and  $\#XMMEA\_EM$  flag, while the pn data were filtered using pattern  $\leq 4$  and  $\#XMMEA\_EP$  flag.

### 2.1.3. NGC 1313 X-2

NGC 1313 X-2 is one example of ULX sources in a nearby spiral galaxy, NGC 1313 ( $D = 3.7$  Mpc). This ULX is located at approximately 8 kpc from the photometric center of the galaxy (Colbert et al. 1995). The data for our analysis were obtained on 2000 October 17 (observation ID 0106860101).

We performed the standard procedures but somehow we failed to create response files for the MOS data, leaving us only the pn data to be analyzed. We set flag = 0 and pattern  $\leq 4$  for the pn-data. Following Miller et al. (2003), we used 24-arcsec radius centered to the source to obtain source spectra, while background counts were extracted in an annulus between 24-arcsec and 30-arcsec.

## 2.2. Fitting Methods

The source spectra were grouped to a minimum of 20 count/bin before fitting using XSPEC version 11.3. We first try the standard spectral model of disk blackbody (DBB) + power-law (PL). We use the results as comparison with other papers. Next, we tried to fit the data by the “*p*-free disk model”, assuming the effective temperature profile of  $T_{\text{eff}} \propto r^{-p}$ , where  $r$  is the disk radius (Mineshige et al. 1994). The *p*-free model is a potentially useful spectral model, since despite its simpleness it is very powerful for discriminating slim disk with  $p \sim 0.5$  from the standard disk with  $p = 0.75$  (Watarai et al. 2000).

We also tried to fit the data with a more sophisticated slim disk model calculated by Kawaguchi (2003), who calculated more realistic emergent spectra of super-critical flow based on the slim disk model, taking into account relativistic and Compton-scattering effects. We will show the results separately apart from those two mentioned above, to avoid muddle, and we will give a brief comment on these results.

The effect of Galactic absorption was taken into account by using wabs model (in XSPEC), where we fixed the value at  $1.5 \times 10^{20} \text{ cm}^{-2}$  for NGC 5204 X-1 and NGC 4559 X-7 and X-10, and  $3.9 \times 10^{20} \text{ cm}^{-2}$  for NGC 1313 X-2 from Dickey and Lockman (1990). The effect of absorption external to our galaxy was also considered and again we used wabs model but we let this value free throughout the fitting.

## 3. Spectral Analysis

The results of spectral analysis for each ULX investigated in this paper will be presented separately for three distinct spectral models: DBB+PL models (in sections 3.1 and 3.2), *p*-free models (in section 3.3), and Kawaguchi’s models (in section 3.4). In addition, we summarize the fitting results in Table 1.

### 3.1. DBB+PL model

We first present our results of fitting based on the conventional approach; i.e., by using the DBB+PL model. As will be explicitly demonstrated below, we will basi-

cally confirm the previous results supporting the IMBH hypothesis.

### 3.1.1. NGC 5204 X-1

We fit the MOS data over 0.3 – 8 keV and the pn data over 0.3 – 10 keV. We obtained a good fit to the data with DBB+PL model (see Fig.1.). The reduced chi-squared is 1.05 with the inner disk temperature,  $kT_{\text{in}} = 0.25 \pm 0.03$  keV, and photon index,  $\Gamma = 1.92 \pm 0.06$ . The low temperature obtained from the fitting apparently supports the IMBH interpretation of ULXs, in agreement with Roberts et al. (2005). The flux obtained from the fitting by using this model is,  $f_x(0.3 - 10 \text{ keV}) = 1.66 \times 10^{-12} \text{ erg cm}^{-2} \text{ s}^{-1}$ . These are in reasonable agreement with the previous results by Roberts et al. (2005); that is,  $kT_{\text{in}} = 0.21 \pm 0.03$  keV, and  $\Gamma = 1.97 \pm 0.07$ .

### 3.1.2. NGC 4559 X-7 and X-10

We next fit both the MOS and the pn data for NGC 4559 X-7 and the pn data for NGC 4559 X-10 over 0.3 – 10 keV. As before, we fit the data with the DBB+PL model and we obtained reduced chi-squared of 0.96 and 0.92 for X-7 and X-10, respectively. The inner disk temperature,  $kT_{\text{in}} = 0.17 \pm 0.09$  keV, and  $\Gamma = 2.17 \pm 0.05$ , were obtained for NGC 4559 X-7, while  $kT_{\text{in}} = 0.48 \pm 0.25$  keV and  $\Gamma = 1.94 \pm 0.13$  were obtained for NGC 4559 X-10. However, for the case of X-10, we could actually obtained a good fit by the PL model alone, giving reduced chi-squared of 0.92 and  $\Gamma = 1.99 \pm 0.03$ .

For reference, the previous fits by Cropper (2004) obtained  $kT_{\text{in}} = 0.148 \pm 0.006$  keV, and  $\Gamma = 2.23 \pm 0.05$  for X-7, in good agreement with our results. As for X-10, Cropper et al. (2004) only shows the fitting result with single component power-law.

### 3.1.3. NGC 1313 X-2

We fit the pn data of NGC 1313 X-2 over 0.2 – 10 keV with the DBB+PL model and found a good fit with reduced chi-squared of 0.96. As in previous cases, we obtain low inner disk temperature,  $kT_{\text{in}} = 0.27 \pm 0.04$  keV, and  $\Gamma = 2.01 \pm 0.13$ .

For comparison, Miller et al. (2003) found  $kT_{\text{in}} = 0.16 \pm 0.16$  keV, and  $\Gamma = 2.3 \pm 0.2$ , for NGC 1313 X-2, from fitting the MOS data with the DBB+PL model. The difference of the detectors is likely the origin of the small discrepancies.

## 3.2. Interpretation based on DBB+PL model

### 3.2.1. Basic methodology to derive black-hole mass

When we obtain a good fit to the observed spectra by the DBB model, we can easily estimate the black-hole mass and the Eddington ratio,  $L/L_E$  (with  $L$  and  $L_E$  being disk luminosity and the Eddington luminosity, respectively), based on the standard disk theory. The basic methodology is summarized in Makishima et al. (2000).

Following Makishima et al. (2000), the bolometric luminosity of an optically thick accretion disk can be written as

$$L_{\text{bol}} = 2\pi D^2 f_{\text{bol}} (\cos i)^{-1} \quad (1)$$

with  $i$  is the inclination of the disk ( $i = 0$  corresponds to face-on geometry) and  $D$  is the distance. This  $L_{\text{bol}}$  is

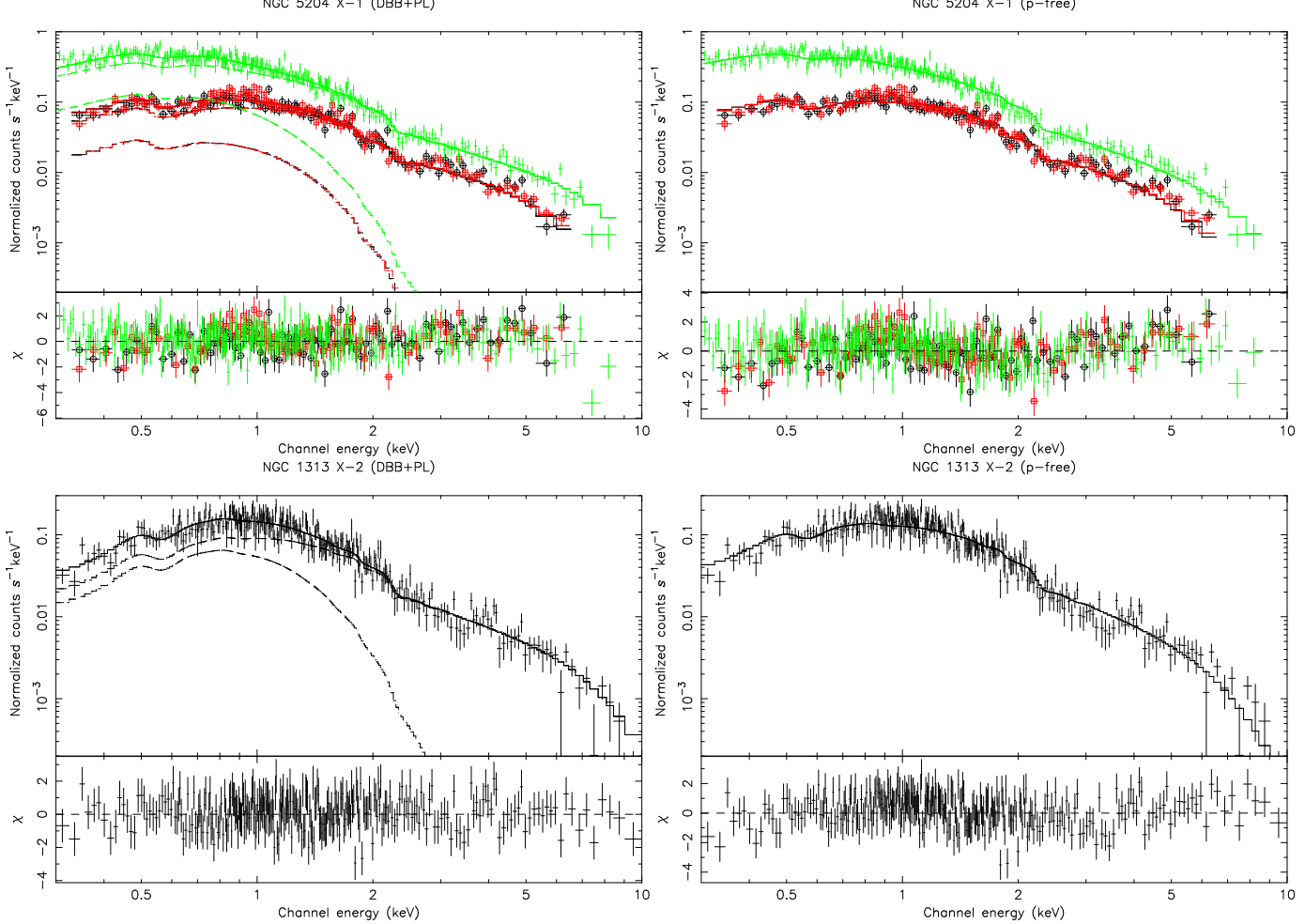


**Fig. 1.** Best fitting spectra and the fit residuals with the DBB+PL model (left panels) and p-free disk model (right panels) for NGC 5204 X-1, NGC 1313 X-2, NGC 4559 X-7 and X-10. Open circles, open squares and dots represent mos1, mos2, and pn data, respectively. Dashed lines in the left panels represent spectral components.

related to the maximum disk color temperature  $T_{\text{in}}$  and the innermost disk radius  $R_{\text{in}}$  as

$$L_{\text{bol}} = 4\pi(R_{\text{in}}/\xi)^2\sigma(T_{\text{in}}/\kappa)^4 \quad (2)$$

where  $\kappa \sim 1.7$  (Shimura, Takahara 1995) is the ratio of the color temperature to the effective temperature, or spectral hardening factor, and  $\xi = 0.412$  is correction factor reflecting the fact that  $T_{\text{in}}$  occurs at somewhat larger than  $R_{\text{in}}$ . Hence, the innermost disk radius is

$$R_{\text{in}} = \xi\kappa^2 \sqrt{\frac{L_{\text{bol}}}{4\pi\sigma T_{\text{in}}^4}} \quad (3)$$

We may identify  $R_{\text{in}}$  with the radius of the last stable Keplerian orbit. Thus, we may in general write

$$R_{\text{in}} = 3\beta R_s = 8.86\beta \left(\frac{M}{M_\odot}\right) \text{ km} \quad (4)$$

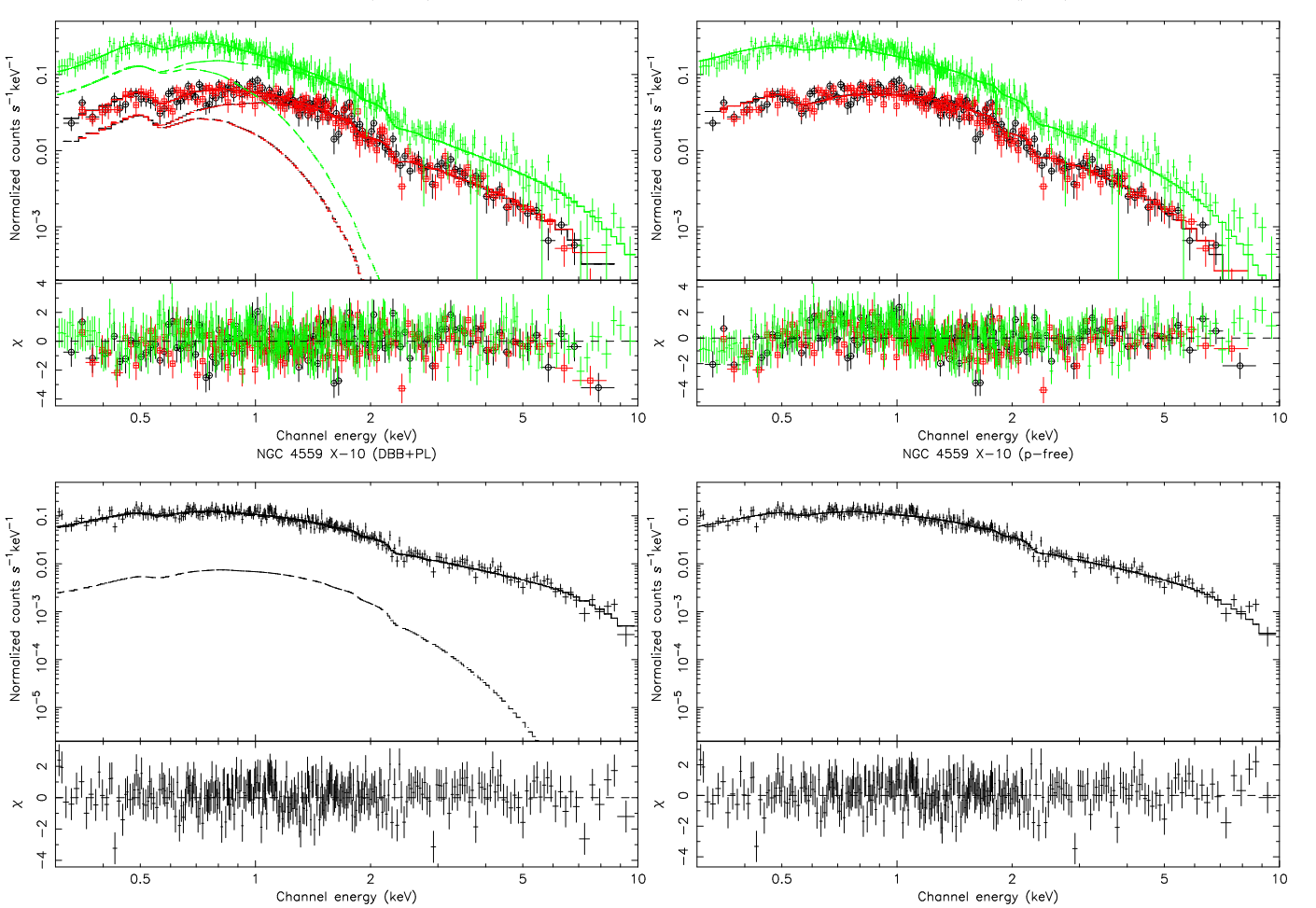
where  $R_s$  is the Schwarzschild radius ( $= 2GM/c^2$ ), by which we can determine the black hole mass. Note that  $1/6 \leq \beta \leq 1$ ,  $\beta = 1/6$  for extremely rotating Kerr black hole and  $\beta = 1$  for Schwarzschild black hole.

Here, we use  $0.3 - 10$  keV flux,  $f_{[0.3-10\text{keV}]}$ , from which we derive  $0.3 - 10$  keV luminosity,  $L_{[0.3-10\text{keV}]}$ . We assume  $L_{\text{bol}} \approx L_{[0.3-10\text{keV}]}$  because all significant energy range from 0.3 to 10 keV. Therefore, using  $T_{\text{in}}$  and  $f_{[0.3-10\text{keV}]}$  from the fitting results, we can determine the value of  $R_{\text{in}}$ , black hole mass, and also  $L_{[0.3-10\text{keV}]}/L_E$ , where  $L_E$  is the Eddington luminosity ( $= 1.5 \times 10^{38}(M/M_\odot)\text{erg s}^{-1}$ ).

### 3.2.2. Problem of DBB+PL model fitting

By using the equations above and the values of  $T_{\text{in}}$  and  $f_{[0.3-10\text{keV}]}$  from the fitting results, we obtained, for the case of NGC 5204 X-1,  $R_{\text{in}} = 2.54 \times 10^3(\cos i)^{-1/2}$  km and the derived black hole mass of  $287\beta^{-1}(\cos i)^{-1/2} M_\odot$ . We also obtained  $L_{[0.3-10\text{keV}]}/L_E = 0.05\beta(\cos i)^{-1/2}$ . In the same way, we obtained relatively large  $R_{\text{in}}$  and hence large black hole mass exceeding  $100 M_\odot$  for other sources (see Table 2).

To summarize, we found through the fitting with the DBB+PL model that the derived black hole masses by far exceed  $100 M_\odot$  and are, hence, within the IMBH regime. Thus, fitting the data with the conventional model supports the idea of sub-critical accretion onto the IMBHs.

Fig. 1. *Continued.*

However, we here point out a serious problem in this interpretation. That is, the spectral decomposition shows that the power-law component predominates in all energy region (see Fig.2 for the case of NGC 5204 X-1). In other words, the disk component only gives a minor contribution in the entire energy ranges for all the sources. Therefore, one is never allowed to use equations (1)–(4), which are derived on the assumption that the radiation is for 100 % from the DBB component. The black hole mass values derived above cannot be so reliable.

### 3.3. *p-free model*

Next, we tried to fit the same data set by the simplified super-critical disk model alone; i.e., the *p*-free disk model.

#### 3.3.1. *Fitting results*

Firstly, we tried the case of NGC 5204 X-1. Surprisingly we also obtained a good fit with this model, although only a single component is considered (see Fig.3). The reduced chi-squared is 1.12. More importantly, we obtained  $p = 0.50 \pm 0.03$ , that is just the value predicted by the theory of super-critical accretion disk (slim disk; Wang, Zhou 1999; Watarai, Fukue 1999). We also obtained high inner disk temperature,  $kT_{\text{in}} = 2.54 \pm 0.34$ , as is expected from

large spectral hardening factors, which the slim disk model predicts.

NGC 5204 X-1 is not an exception (see Table 1). We also found a good fit with the *p*-free model for the cases of NGC 4559 X-7 and X-10. The *p* values of  $0.50 \pm 0.03$  (X-7) and  $0.51 \pm 0.06$  (X-10) and the inner disk temperatures of  $1.84 \pm 0.16$  keV (X-7) and  $3.16 \pm 0.71$  keV (X-10) are again consistent with the slim disk model.

As for the cases of NGC 1313 X-2, fitting with the *p*-free model only also gave a good fit. We obtained,  $kT_{\text{in}} = 2.00 \pm 0.34$  keV, and the *p*-value is  $0.50 \pm 0.05$ .

#### 3.3.2. *Interpretation of p-free model*

It is clear from the results of the fitting with *p*-free model that the obtained *p* value is around 0.5, indicating super-critical accretion flow (slim disk) for all the data. Applying similar interpretation as in the case of fitting with DBB+PL, we obtained,  $R_{\text{in}} = 23.7(\cos i)^{-1/2}(\kappa/1.7)^2$  km, the derived black hole mass of  $2.67\beta^{-1}(\cos i)^{-1/2}(\kappa/1.7)^2 M_{\odot}$  and  $L_{[0.3-10\text{keV}]}/L_{\text{E}} = 5.29\beta(\cos i)^{-1/2}(\kappa/1.7)^{-2}$  for NGC 5204 X-1.

Caution is needed here, however, regarding the inner edge of the disks in the slim disk regimes and the plausible spectral hardening factor values ( $\kappa$ ). Through the

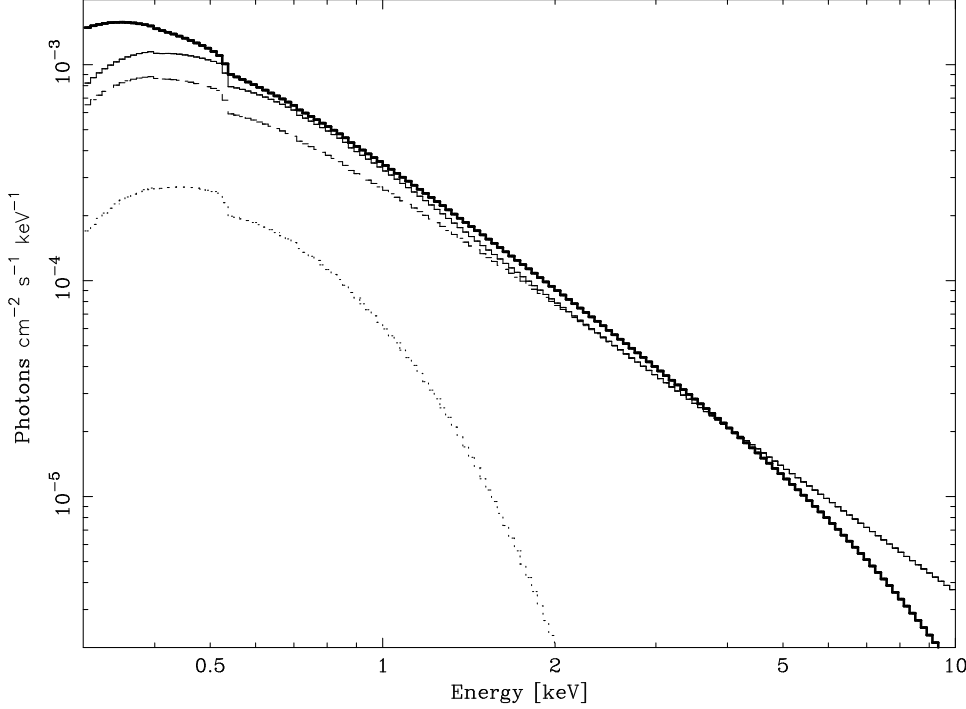


**Fig. 2.** Spectral decompositions of the fits for NGC 5204 X-1. The thinner lines represent, from bottom to top, disk component, power-law component, and total component, while the thicker line represents p-free model

careful numerical integration, Watarai et al. (2000) found that the inner edge of the disk is substantially smaller,  $R_{\text{in}} \sim R_S$  (i.e.,  $\beta \sim 1/3$ ), in the slim disk regime, compared with that in sub-critical (standard disk) regime,  $R_{\text{in}} \sim 3R_S$  ( $\beta \sim 1$ ), even though a central black hole is not rotating. This is because enhanced mass accretion flow with high density finally fills up an empty zone inside  $3R_S$ , which exists in the sub-critical accretion regimes. We then expect significant blackbody emission from inside  $3R_S$ . It is thus preferable to set  $\beta \sim 1/3$ , instead of  $\beta = 1$ . However, radiation from the vicinity of black holes should be attenuated because of intense gravitational redshifts and transverse Doppler effect, and since the effective temperature corrected for the relativistic effect has a peak at around  $2R_S$ ,  $\beta \sim 2/3$  will be a more reasonable estimate (Kawaguchi 2003).

As for the spectral hardening factor, Shimura and Takahara (1995) and Zampieri et al. (2001) found  $\kappa \approx 1.7$  for stellar-mass black holes, and it increases with increasing  $\dot{M}$ . In the slim disk, the disk temperature gets higher and the density becomes smaller as  $\dot{M}$  increases, therefore the electron scattering becomes more dominant and the spectral hardening factor becomes much higher than  $\sim 1.7$  (Kawaguchi 2003). Watarai and Mineshige (2003) found from the comparison between the limit-cycle instability theory (Honma et al. 1991) and the observation of GRS1915+105 that the spectral hardening factor close to the Eddington luminosity should be about 3.

The mass estimated from the  $p$ -free models is proportional to  $\kappa^2$ , so if we take a larger  $\kappa$ , say, 3, the inferred

mass will be tripled compared to the case of standard disks ( $\kappa \sim 1.7$ ). Consequently, adopting  $\beta \sim 2/3$ , our mass estimate is  $12.5(\cos i)^{-1/2}(\kappa/3.0)^2 M_\odot$  and the Eddington ratio is  $L_{[0.3-10\text{keV}]}/L_E \sim 1.1(\cos i)^{-1/2}(\kappa/3.0)^{-2}$  for NGC 5204 X-1. In the same manner, we find smaller black hole masses and larger Eddington ratios for other sources (see Table 2). The derived black hole mass is well within the stellar mass black hole regime.

#### 3.4. Fitting Results with Kawaguchi's model

Finally, we present the results of the data fitting with the slim disk model developed by Kawaguchi (2003) (see Foschini et al. 2005 for the case of ULX M33 X-8). He developed several models, but we chose the model in which the effects of electron scattering and relativistic correction are included. Calculation was made and fitting was tried for several different values of the viscous parameter,  $\alpha$ . We found  $\alpha = 0.1$  gives most satisfactory fits, and will show only the results with  $\alpha = 0.1$  in this paper. Source distance was fixed, and the face-on geometry assumed. Model parameters are only mass and mass accretion rate (in the unit of  $L_{\text{Edd}}/c^2$ ). We summarize the fitting results using this model in Table 3.

The best fit for NGC 5204 X-1 was obtained with reduced chi-squared of 1.18, black hole mass of  $18M_\odot$  and mass accretion rate of  $27\dot{M}_{\text{Edd}}$ , where  $\dot{M}_{\text{Edd}} \equiv L_{\text{Edd}}/c^2$ <sup>1</sup>. All the analyzed data of ULXs can be fitted with

<sup>1</sup> Here,  $16L_{\text{Edd}}/c^2$  is the critical accretion rate, which would pro-

**Table 1.** Fitting results with DBB+PL and  $p$ -free model.  $N_{\text{H}}$  is an absorption column external to our Galaxy in unit of  $10^{21}$  atom  $\text{cm}^{-2}$ . A Galactic absorption column is assumed as in the text.  $kT_{\text{in}}$  is the inner disk temperature in keV. The normalization for DBB and  $p$ -free is defined by  $[(R_{\text{in}}/\text{km})/(D/10\text{kpc})]^2 \cos i$ , where  $R_{\text{in}}$  is the inner disk radius,  $D$  the distance to the source, and  $i$  the angle of the disk. The unit of power-law normalization is photon/s/cm<sup>2</sup>/keV at 1 keV.  $f_{\text{x}}$  is the observed flux in units of erg  $\text{cm}^{-2} \text{ s}^{-1}$  (0.3 – 10 keV) that depends on the model.

Parameter	NGC 5204 X-1	NGC 4559 X-7	NGC 4559 X-10	NGC 1313 X-2
DBB+PL				
$N_{\text{H}}$	$0.51 \pm 0.11$	$1.58 \pm 0.19$	$0.98 \pm 0.22$	$1.98 \pm 0.27$
$kT_{\text{in}}$	$0.25 \pm 0.03$	$0.17 \pm 0.09$	$0.48 \pm 0.25$	$0.27 \pm 0.04$
Norm.	$3.7 \pm 2.6$	$46.9 \pm 30.3$	$0.04 \pm 0.11$	$4.5 \pm 4.0$
$\Gamma$	$1.92 \pm 0.06$	$2.17 \pm 0.05$	$1.94 \pm 0.13$	$2.01 \pm 0.13$
Norm.	$(3.02 \pm 0.48) \times 10^{-4}$	$(2.10 \pm 0.24) \times 10^{-4}$	$(2.01 \pm 0.83) \times 10^{-4}$	$(2.02 \pm 0.73) \times 10^{-4}$
$f_{\text{x}}$	$1.66 \times 10^{-12}$	$8.36 \times 10^{-13}$	$9.42 \times 10^{-13}$	$8.63 \times 10^{-13}$
$\chi^2/\text{dof}$	1.05	0.96	0.93	0.98
p-free				
$N_{\text{H}}$	$0.34 \pm 0.01$	$0.60 \pm 0.06$	$0.91 \pm 0.08$	$1.42 \pm 0.14$
$kT_{\text{in}}$	$2.54 \pm 0.34$	$1.84 \pm 0.16$	$3.16 \pm 0.71$	$2.03 \pm 0.35$
$p$	$0.50 \pm 0.03$	$0.50 \pm 0.03$	$0.51 \pm 0.06$	$0.50 \pm 0.05$
Norm.	$(5.04 \pm 6.11) \times 10^{-4}$	$(1.04 \pm 0.85) \times 10^{-3}$	$(1.51 \pm 3.13) \times 10^{-4}$	$(8.13 \pm 12.9) \times 10^{-4}$
$f_{\text{x}}$	$1.55 \times 10^{-12}$	$7.96 \times 10^{-13}$	$9.14 \times 10^{-13}$	$8.08 \times 10^{-13}$
$\chi^2/\text{dof}$	1.12	1.19	0.93	1.15

Kawaguchi's model and the derived black hole masses are less than  $100 M_{\odot}$  (see Table 3). This is not so surprising for the data showing the slim disk signatures, because the basic spectral shapes of his model are similar to those of the  $p$ -free model with  $p \sim 0.5$  (as long as  $\dot{M} \gg L_{\text{E}}/c^2$ ).

## 4. Discussion

### 4.1. Accretion Disk Models and Black Hole Mass

In the present study, we re-examined the XMM-Newton data of ULXs through the conventional and more sophisticated spectral models constructed based on the theoretical study of super-critical accretion flow. We would like to comment on the results from fitting with DBB+PL and  $p$ -free model first. It is obvious from the fitting results in other papers, e.g. Roberts et al. (2005), Cropper et al. (2004), Miller et al. (2003,2004), that the DBB+PL model provides a good fit to several ULXs data, and the 'cool' disk temperature obtained from the fitting suggests an existence of IMBHs inside the ULXs. However, we should note that this is only one option, and we tried another option; namely, the  $p$ -free model. Remarkably, the  $p$ -free model also gives good fit to the same data. Moreover, the

duce Eddington luminosity in the case of a classical radiative efficiency (1/16).

obtained  $p$  values, which are  $\sim 0.5$ , indicating the super-critical accretion (slim disk) model, in stead of standard disk (DBB) model where,  $p = 0.75$ . The derived black hole masses and the Eddington ratios also support this conclusion.

Why can the two distinct models give similarly good fits to the data? A trick lies in the spectral slope of the slim disk model. For a power-law temperature profile,  $T \propto r^{-p}$ , the entire disk spectra, which is the summation of the blackbody emission spectra from various radii, give power-law spectral slope in the intermediate energy range (below  $h\nu < kT_{\text{in}}$ ) with a spectral slope of  $F_{\nu} \propto \nu^{3-(2/p)}$  (see, e.g., chapter 3 of Kato et al. 1998). Then, a photon index is  $\Gamma = (2/p) - 2$ . That is, for a slim disk with  $p = 1/2$ , we have  $\Gamma = 2$ . (Note that for a standard disk with  $p = 3/4$  we get  $\Gamma = 2/3$ .) This is a striking coincidence that both of the PL model with  $\Gamma = 2$  and the slim disk model give the same power-law spectra in the moderate energy range. To see this more explicitly, we show in Fig. 2 the two fitting models with fitting parameters obtained for NGC 5204 X-1. We see that both DBB+PL model and slim disk model produce power-law decline with a power-law index  $\sim -1$  (or photon index,  $\Gamma \sim 2$ ) and are identical at 0.5  $\sim$  5 keV energy range.

In the present paper, it was hardly possible from model fitting to judge if the DBB+power-law model or the slim disk model is preferred, being limited by photon statistics. It is, however, in principle possible to distinguish the

**Table 2.** The derived black hole mass value from DBB+PL model and  $p$ -free model in  $M_{\odot}$  and the ratio between luminosity at 0.3 – 10 keV and Eddington luminosity. We assumed  $\beta \sim 1$  for DBB+PL model and  $\beta \sim 2/3$  for  $p$ -free model (see text). The spectral hardening factor,  $\kappa$ , is assumed to be 1.7 for DBB model, and considered to be  $\approx 3$  for slim disk.

	NGC5204 X-1	NGC4559 X-7	NGC4559 X-10	NGC1313 X-2
DBB+PL				
$M(\cos i)^{1/2}$	287	889	118	136
$L(\cos i)^{1/2}/L_E$	0.05	0.03	0.3	0.03
$p$ -free				
$M(\cos i)^{1/2}$	$12.5(\frac{\kappa}{3})^2$	$34.6(\frac{\kappa}{3})^2$	$12.5(\frac{\kappa}{3})^2$	$11.2(\frac{\kappa}{3})^2$
$L(\cos i)^{1/2}/L_E$	$1.1(\frac{\kappa}{3})^{-2}$	$0.9(\frac{\kappa}{3})^{-2}$	$2.8(\frac{\kappa}{3})^{-2}$	$0.4(\frac{\kappa}{3})^{-2}$

**Table 3.** Fitting results with slim disk model of Kawaguchi (2003).  $N_H$  is an absorption column external to our Galaxy in unit of  $10^{21}$  atom cm $^{-2}$ . A Galactic absorption column is assumed as in the text.  $M$  is mass in  $M_{\odot}$ .  $\dot{M}$  is mass accretion rate ( $= L_{\text{Edd}}/c^2$ ).  $f_x$  is the observed flux in units of  $10^{-12}$  erg cm $^{-2}$  s $^{-1}$  (0.3 – 10 keV) that depends on the model.

Fit Par.	NGC5204 X-1	NGC4559 X-7	NGC4559 X-10	NGC1313 X-2
$N_H$	$0.09 \pm 0.03$	$0.45 \pm 0.03$	$0.69 \pm 0.07$	$1.23 \pm 0.07$
$M$	$18^{+2}_{-2}$	$57^{+4}_{-4}$	$24^{+9}_{-7}$	$12^{+1}_{-1}$
$\dot{M}$	$27^{+5}_{-4}$	$18^{+2}_{-1}$	$100^{+70}_{-40}$	$14^{+2}_{-1}$
$f_x$	1.6	0.79	0.91	0.8
$L_{[0.3-10\text{keV}]}/L_E$	0.81	0.52	1.42	0.36
$\chi^2/\text{dof}$	1.18	1.20	0.93	1.17

two models by measuring their spectra very accurately. So far, XMM-Newton has been able to do this only for M82 X-1, the brightest ULX (Okajima et al. 2006). Okajima et al. (2006) found that the energy spectrum of M82 X-1 above  $\sim 3$  keV has a curvature just between the power-law and DBB model, and is represented pretty well with  $p$ -free model of  $p=0.61$ . This is considered to be strong evidence of slim disk in ULXs. Next generation hard X-ray satellites with higher sensitivity and imaging capability are expected to precisely measure the energy spectra of most ULXs, so that black hole parameters are constrained by applying precise slim disk model spectra.

#### 4.2. Luminosity-Temperature diagram

Then, which is more likely the case, sub-critical accretion onto intermediate-mass black holes or super-critical accretion onto stellar-mass black holes?

We pointed out a serious problem inherited from the DBB+PL model. The spectral fitting with DBB+PL model shows that the power-law component predominates in all energy regions (Fig. 2). In other words, disk contribution is very small compared to the power-law contribution and therefore the black hole masses derived above might not be so reliable, because the standard disk relations cannot be used here.

On the other hand, a good fit with  $p$ -free model alone implies that the disk contributes in all energy region, therefore, the black hole masses derived from the fitting

with  $p$ -free model can be reliable. For these reasons, we can safely conclude that the latter model is more likely the case to explain the physics of ULXs.

We summarize our results in Fig. 3. This is the temperature-luminosity diagram (cf. Makishima et al. 2000; cf. Miller et al. 2004) with the lines of constant black-hole masses. We plot our ULXs fitting results with DBB+PL and  $p$ -free model together with several best-studied stellar-mass black hole candidates (BHCs). We can see that the low temperatures obtained from the fitting using the DBB+PL model are shifted to higher temperatures when fitted with the  $p$ -free model. This implies that the black hole mass values in the range of IMBHs obtained from the fitting with the DBB+PL model can be shifted to the stellar mass range by the  $p$ -free model; that is, still there is no evidence of IMBHs so far, at least in four ULXs investigated in this paper, due to the minor disk contribution in DBB+PL model as mentioned before.

It then naturally follows that all the fitting results which gave low disk temperatures and photon indices of  $\Gamma \sim 2$  should be re-examined, since those data are very likely to be fitted with the slim disk ( $p$ -free) model equally well. Obviously, the latter model gives higher disk temperatures and hence lower black hole masses. It is, in this respect, interesting to note the statistical study of ULXs by Winter et al. (2006) who examined distribution of photon indices and found a concentration at  $\Gamma \sim 2$  for the high-state ULXs, those ULXs whose spectra can well be

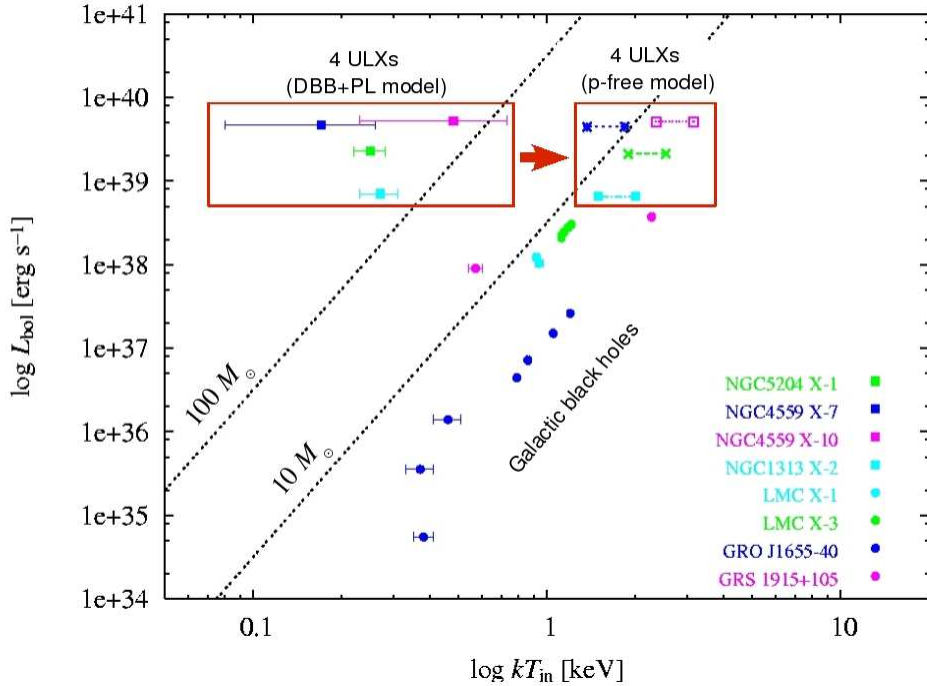


**Fig. 3.** Relation between the luminosity at  $0.3 - 10$  keV ( $L_{[0.3-10\text{keV}]}$ ) and  $T_{\text{in}}$  for ULXs and stellar mass black hole candidates (BHCs). BHCs references: Ebisawa 1991 (LMC X-1), Treves et al. 1988 (LMC X-3), Mendez et al. 1998 (GRO J1655-40), and Belloni et al. 1997 (GRS 1915+105). Note that in this figure  $L_{\text{bol}}$  means the  $0.3 - 10$  keV luminosity for ULXs and the bolometric luminosity for Galactic black hole candidates, both assuming the face-on geometry. The ranges of  $T_{\text{in}}$  in the  $p$ -free model box represent the values via DBB model (lowest end) and  $p$ -free model (highest end).

fitted with the combined DBB+PL model. Some of them may be in the slim disk regimes, rather than in the high state.

## 5. Conclusion

We have investigated the XMM-Newton EPIC spectra of the four ULXs which were claimed as strong candidates of IMBHs by several authors. We found that these spectra are successfully fitted with slim disk models, and the derived masses are  $\sim 11$  to  $60 M_{\odot}$  depending on different assumptions. We have not seen the evidence of the “intermediate mass” black holes having several hundreds of  $M_{\odot}$ . When mass accretion rate is close to or exceeding the critical rates, the slim disk is theoretically predicted. We suggest that ULXs are stellar mass black holes, at most several tens of  $M_{\odot}$  under super-critical accretion rates shining at super-Eddington luminosities.

We gratefully thank Marek Abramowicz for valuable comments and suggestions. This work was supported in part by the Grants-in-Aid of the Ministry of Education, Science, Culture, and Sport (14079205, 16340057 S.M.), by the Grant-in-Aid for the 21st Century COE “Center for

Diversity and Universality in Physics” from the Ministry of Education, Culture, Sports, Science and Technology (MEXT) of Japan. K.V. gratefully thank Ken-ya Watarai for the discussions at some beginnings of this work and also MEXT scholarship. T.K. thanks the financial supports from JSPS Postdoctoral Fellowship (01879).

## References

- Abramowicz, M. A., Jaroszynski, M., & Sikora, M. 1978, A&A, 63, 221
- Abramowicz, M. A., Calvani, M., & Nobili, L. 1980, ApJ, 242, 772
- Abramowicz, M. A., Czerny, B., Lasota, J. P., & Szuszkiewicz, E. 1988, ApJ, 332, 646
- Abramowicz, M. A., Kato, S., & Matsumoto, R. 1989, PASJ, 41, 1215
- Abramowicz, M. A., Klužniak, W., McClintock, J. E., & Remillard, R. A. 2004, ApJ, 609, L63
- Belloni, T., Méndez, M., King, A. R., van der Klis, M., & van Paradijs, J. 1997, ApJ, 479, L145
- Colbert, E. J. M., Petre, R., Schlegel, E. M., & Ryder, S. D. 1995, ApJ, 446, 177
- Colbert, E. J. M., & Ptak, A. F. 2002, ApJS, 143, 25
- Cropper, M., Soria, R., Mushotzky, R. F., Wu, K., Markwardt, C., B., & Pakull, M. 2004, MNRAS, 349, 39

Davis, S. W., Done, C., & Blaes, O. M. 2006, astro-ph/0602245

Dickey, J. M., & Lockman, F. J. 1990, *ARA&A*, 28, 215

Ebisawa, K., Mitsuda, K., & Hanawa, T. 1991, *ApJ*, 367, 213

Ebisawa, K., Makino, F., Mitsuda, K., Belloni, T., Cowley, A. P., Schmidtke, P. C., & Treves, A. 1993, *ApJ*, 403, 684

Ebisawa, K., Źycki, P., Kubota, A., Mizuno, T., & Watarai, K. 2003, *ApJ*, 597, 780

Fabbiano, G. 1989, *ARA&A*, 27, 87

Foschini, L., et al. 2005, astro-ph/0506298

Gierliński, M., Maciołek-Niedźwiecki, A., & Ebisawa, K. 2001, *MNRAS*, 325, 1253

Honma, F., Kato, S., & Matsumoto, R., 1991, *PASJ*, 43, 147

Kato, S., Fukue, J., Mineshige, S. 1998, *Black-Hole Accretion Disks* (Kyoto: Kyoto University Press)

Kawaguchi, T. 2003, *ApJ*, 593, 69

King, A. R. 2004, *MNRAS*, 347, L18

King, A. R., Davies, M. B., Ward, M. J., Fabbiano, G., & Elvis, M. 2001, *ApJ*, 552, L109

Körding, E., Falcke, H., & Markoff, S. 2002, *A&A*, 382, L13

Lachowicz, P., Czerny, B., & Abramowicz, M. A. 2006, astro-ph/0607594

Madhusudhan, N., Justham, S., Nelson, L., Paxton, B., Pfahl, E., Podsiadlowski, Ph., & Rappaport, S. 2006, *ApJ*, 640, 918

Makishima, K., et al. 2000, *ApJ*, 535, 632

McClintock, J. E., & Remillard, R. A. 2003, astro-ph/0306213

McClintock, J. E., Shafee, R., Narayan, R., Remillard, R. A., Davis, S. W., & Li, L. X. 2006, astro-ph/0606076

Méndez, M., Belloni, T., & van der Klis, M. 1998, *ApJ*, 499, L187

Miller, J. M., Fabbiano, G., Miller, M. C., & Fabian, A. C. 2003, *ApJ*, 585, L37

Miller, J. M., Fabian, A. C., & Miller, M. C. 2004, *ApJ*, 614, L117

Mineshige, S., Hirano, A., Kitamoto, S., Yamada, T. T., & Fukue, J. 1994, *ApJ*, 426, 308

Mucciarelli, P., Casella, P., Belloni, T., Zampieri, L., & Ranalli, P. 2006, *MNRAS*, 365, 1123

Okajima, T., Ebisawa, K. & Kawaguchi, T. 2006, *ApJL*, submitted

Pakull, M. W & Mirioni, L. 2002, astro-ph/0202488

Ptak, A. & Colbert, E. 2004, *ApJ*, 606, 291

Reynolds, C. S., Loan, A. J., Fabian, A. C., Makishima, K., Brandt, W. N., & Mizuno, T. 1997, *MNRAS*, 286, 349

Roberts, T. P., Warwick, R. S., Ward, M. J., Goad, M. R., & Jenkins, L. P. 2005, *MNRAS*, 357, 1363

Roberts, T. P., & Warwick, R. S. 2000, *MNRAS*, 315, 98

Shafee, R., McClintock, J. E., Narayan R., Davis, S. W., Li, L. X., & Remillard, R. A. 2006, *ApJ*, 636, L113

Shimura, T., & Takahara, F. 1995, *ApJ*, 445, 780

Strohmayer, T. E., & Mushotzsky, R. F. 2003, *ApJ*, 586, L61

Török, G. 2005, *A&A*, 440, 1

Treves, A., Belloni, T., Chiappetti, L., Maraschi, L., Stella, L., Tanzi, E. G., & van der Klis, M. 1988, *ApJ*, 325, 119

Wang, D. Q. 2002, *MNRAS*, 332, 764

Wang, J. M., & Zhou, Y. Y. 1999, *ApJ*, 516, 420

Watarai, K., & Fukue, J. 1999, *PASJ*, 51, 725

Watarai, K., Fukue, J., Takeuchi, M., & Mineshige, S. 2000, *PASJ*, 52, 133

Watarai, K. & Mineshige, S. 2003, *ApJ*, 596, 421

Watarai, K., Mizuno, T., & Mineshige, S. 2001, *ApJ*, 549, L77

Winter, L.M., Mushotzky, R. F., & Reynolds, C. S. 2005, astro-ph/0512480

Zampieri, L., Turolla, R., & Szuszkiewicz, E. 2001, *MNRAS*, 325, 1266